Combined Ring Inversion and Side Group Rotation in Geminal Diphosphoryl Substituted Pyrrolidinoxyl Radicals: ESR Analysis of Chemical Exchange between Four Nonequivalent Sites†

Antal Rockenbauer,‡ Anne Mercier,§ François Le Moigne,§ Gilles Olive,§ and Paul Tordo*,§

Central Research Institute for Chemistry, H-1525 Budapest, P.O. Box 17, Hungary, Technical University of Budapest, H-1111 Budapest, Budafoki u. 8., Hungary, and Laboratoire Structure et Réactivité des Espèces Paramagnétiques, Boite 521, CNRS UMR 6517 "Chimie, Biologie et Radicaux Libres", Universités d'Aix-Marseille I et III, Centre de St Jérôme, Avenue Escadrille Normandie-Niemen, 13397 Marseille Cedex 20, France

Received: January 23, 1997; In Final Form: June 17, 1997⊗

The ESR spectra of three diphosphorylated pyrrolidinoxyl radicals have been studied over a large temperature range. While for the trans 2,5-disubstituted compound **1** no line width alternation was found, for the 2,2-disubstituted compounds **2** and **3**, dramatic changes in the spectra were observed as a function of the temperature. These changes were explained by a four-site chemical exchange model including both ring inversion and hindered rotation around the carbon−phosphorus bonds. For radical **3**, the presence of additional 5,5-dimethyl substitution can completely block rotations around carbon−phosphorus bonds for certain ring geometries, while for other ring conformations chemical exchange still occurs through combined inversion−rotation processes. An effective two-site model composed of nonequivalent sites and a superposition model composed of a pair of exchanging conformers and a pair of nonexchanging conformers were used to simulate spectrum variations. A satisfactory fit was obtained over the entire temperature range investigated. From the temperature dependence of the exchange frequencies the potential barriers for ring inversion (27 kJ/mol), for combined inversion−rotation (11 kJ/mol), and for rotation around the carbon−phosphorus bonds (14 kJ/mol) were estimated.

Introduction

We have shown[1] previously that in the series of β-phosphorylated five-membered-ring nitroxides the ESR phosphorus coupling was very sensitive to the ring conformation and represented a valuable structural probe (Scheme 1).

This observation led us to develop the synthesis and the use[1b,2] of new nitrones which would trap free radicals to generate β-phosphorylated five-membered-ring nitroxide spin adducts (Scheme 2).

When Y = $P(O)(OR)_2$, the previously unknown 2,2- or 2,5-diphosphorylated pyrrolidinoxyl radicals were detected, and some of these radicals exhibited ESR spectra showing dramatic changes with temperature. In the present paper we describe the generation and the ESR study over a large temperature range of nitroxides **1**−**3** (Scheme 3).

The very unusual temperature effects observed in the ESR spectra of **3** (Figure 1) will be discussed and analyzed in terms of a nonequivalent four-site chemical exchange model.

Nitroxides **1**, **2**, and **3** were generated as shown in Scheme 4.

The few cases of four-site chemical exchange processes reported in the literature[3] deal with the exchange of hydrogen atoms between sites having different proton hyperfine interactions. In the case described hereafter the difference in hyperfine interactions for the exchanging phosphorus nuclei in the different sites is much larger than for protons. Since line broadening is proportional to the square of the difference of the hyperfine coupling for the exchanging sites, an enhancement of exchange effects can be expected. This enhancement should allow the investigation of intramolecular motions over a broader frequency range since, in such cases, a very fast exchange rate is needed to average out the large difference in coupling constants. For

SCHEME 1

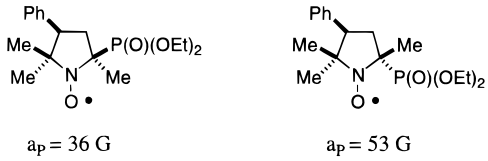

a_P = 36 G a_P = 53 G

SCHEME 2

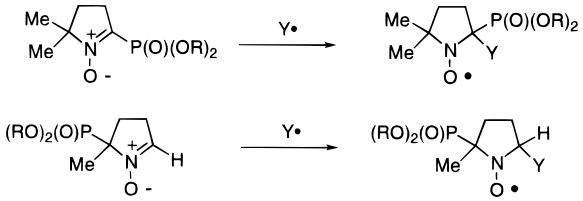

SCHEME 3

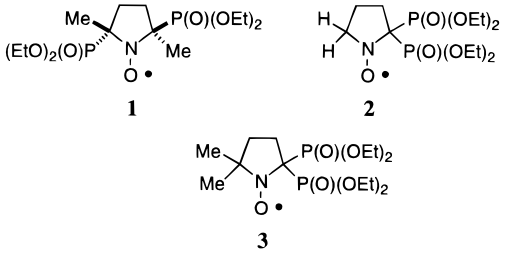

1 **2**

3

† This paper is dedicated to Professor Fabian Gerson for his invaluable contribution to the ESR of organic radicals.

‡ Central Research Institute for Chemistry and Technical University of Budapest.

§ Universités d'Aix-Marseille I et III.

* Author to whom all correspondence should be addressed.

⊗ Abstract published in *Advance ACS Abstracts,* September 15, 1997.

S1089-5639(97)00298-3 CCC: $14.00

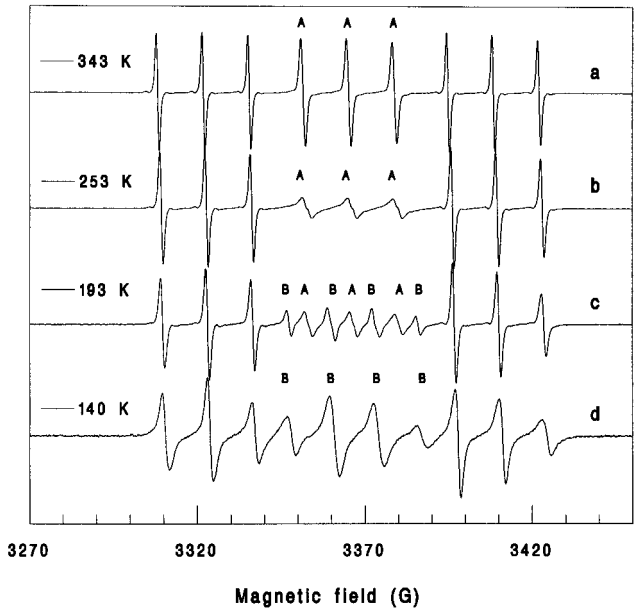

Figure 1. ESR spectra of radical **3**: (a) 343 K, (b) 253 K, (c) 193 K, and (d) 140 K.

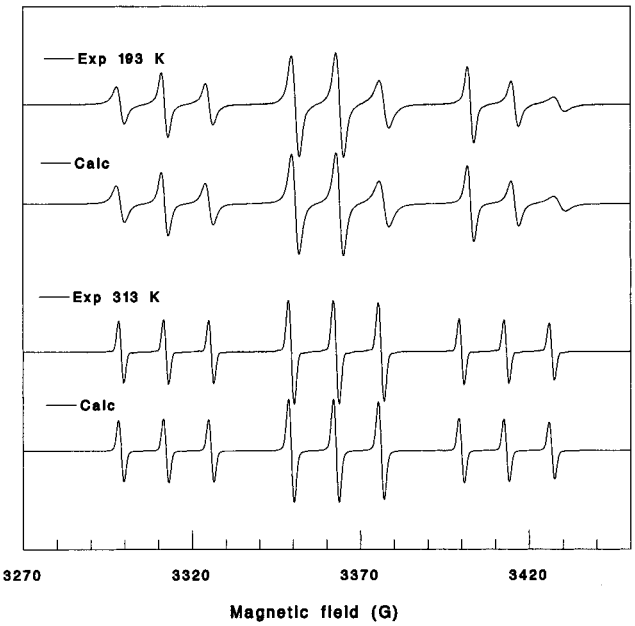

Figure 2. Experimental and calculated ESR spectra of radical **1**: 193 K (top) and 313 K (bottom).

SCHEME 4

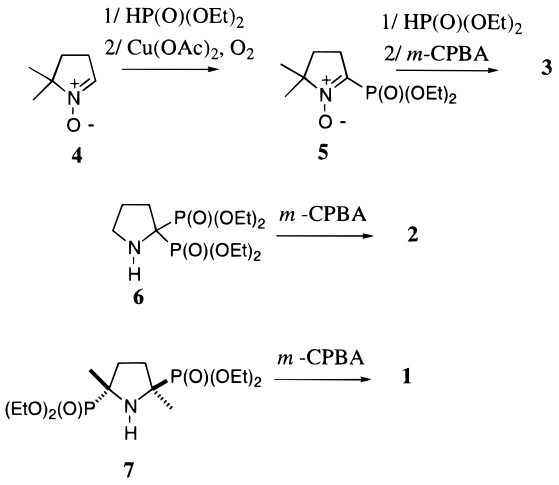

example for five-membered rings, fast ring inversion usually prevents any line width alternation;[4] however, the presence of large phosphorus couplings could allow ring inversion to be detected. Moreover rotations around the carbon−phosphorus bonds can influence the ring conformation and thus the phosphorus couplings. If the rotations are slow due to the strong steric interactions between geminal substituents, a significant line width broadening could occur allowing the study of two coupled dynamic processes: rotation around the carbon−phosphorus bonds and ring inversion.

Quantitative information about exchange rates was obtained applying the modified Bloch equations[5] to describe line shapes. An automatic parameter adjustment technique was developed to achieve optimum fits.[6] At low temperature, where viscosity is high, relaxation broadening due to magnetic anisotropies hinders the precise determination of exchange rates. To separate line broadening resulting from chemical exchange or relaxation phenomena, we compared data obtained in solvents with different viscosity (toluene, cyclopropane, and dichloromethane). Besides geminally substituted radicals we also investigated the 2,5-trans diphosphorylated molecule **1** to see the influence of less hindered rotations around the carbon−phosphorus bond.

Results

ESR Spectra. At high temperature the ESR spectra of isomers **1** (Figure 2) and **3** (Figure 1a) show the same hyperfine pattern, which consists of a large triplet assignable to the equivalent phosphorus nuclei, each line of the main triplet being split into a 1:1:1 triplet due to the nitrogen coupling. While for **1** (Figure 2) the amplitude ratio in the phosphorus triplet is 1:2:1 over the entire temperature range, for **3** the inner line has a smaller amplitude even at high temperatures. By lowering the temperature the amplitudes of the inner lines diminish further in the spectra of **3**, and at 253 K they split to doublets with separation of ca. 2 G (Figure 1b). These lines will be called A type lines, and they can be accounted for by the existence of two slightly different phosphorus couplings. Upon decreasing the temperature further, a new set of lines denoted as B appears in the center of the spectra (Figure 1c), and they can be accounted for by the existence of two nonequivalent phosphorus nuclei exhibiting strongly different couplings. The relative intensity of the B lines compared to the A lines increases at low temperature, and finally below 153 K (Figure 1d), the A lines vanish, these spectral changes being completely reversible.

The ESR spectra of **2** exhibit an additional triplet splitting due to the 5,5′ protons (see lines A in Figure 3), and at high temperature a pattern of 27 well-resolved lines can be detected. The inner lines of the ^{1}H and ^{31}P triplets (the latter are denoted by A′ in Figure 3) have smaller amplitude than the expected 1:2:1 theoretical ratio, the broadening being larger for the ^{31}P triplets. Upon decreasing the temperature the exchange broadening becomes larger, and around 200 K in dichloromethane new lines (see B and B′ lines in Figure 3) appear close to the inner line of the ^{1}H and ^{31}P triplets.

Simulation of ESR Spectra. For radical **1** no chemical exchange was considered, and only relaxational broadening of the nitrogen and phosphorus triplets was taken into account. For radicals **2** and **3** both chemical exchange and relaxational broadening were considered. In the high-temperature region the line shape is strongly affected by unresolved long-range proton couplings, and some resolution can be seen for **2**; therefore, we also considered the couplings of all methyl and methylene protons of the ring. When the resolution was good, the satellite lines of naturally abundant ^{13}C isotopes were also simulated by considering the couplings of α and methyl carbons.

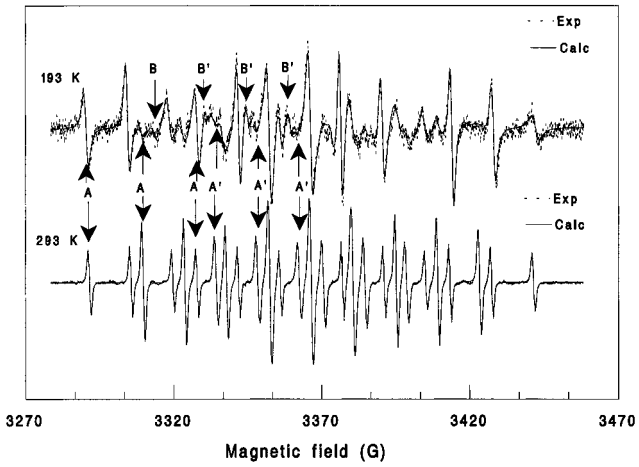

Figure 3. Experimental and calculated ESR spectra of radical **2** recorded at 193 K (top) and 293 K (bottom). The A and B lines are indicated by arrows.

SCHEME 5

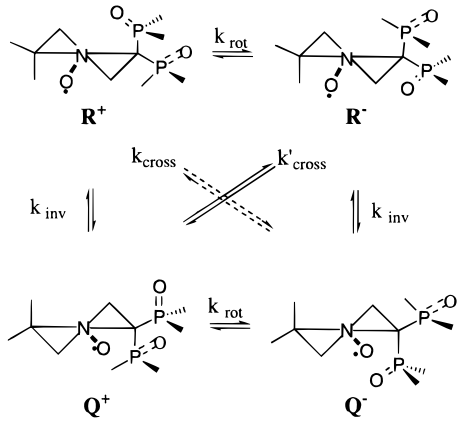

Chemical Exchange Network. To characterize a network of molecular interconversions, we tentatively assume that ring inversion takes place between conformations Q and R, while the geminal phosphoryl groups have a gear rotation between states + and − (Scheme 5). Accordingly exchange can take place between four conformers: Q^+ , Q^-, R^+, and R^-, respectively, where the Q^+, R^- and Q^-, R^+ pairs are mirror images. The Q and R conformations can generally be represented by more or less distorted $^4T_3$ and $^3T_4$ conformers. Due to their strong steric interaction, the rotation of phosphoryl groups in the geminal position is not independent, and some kind of gear motion is expected. The R^+ and Q^- conformers, which have an axial phosphorus group with its P═O bond pointing toward the ring, are energetically favored. We can define a + state as a state that has a minimum steric interaction in the $^4T_3$ conformation, while the same condition holds for a − state in the $^3T_4$ conformation.

Four rate constants describe the whole exchange network (Scheme 5): k_{inv} for the ring inversion between Q and R, k_{rot} for the rotation between + and −, k_{cross} and k_{cross}' for the cross-exchanges between pairs of mirror images (Q^+, R^-) and (Q^-, R^+), respectively. Note that k_{cross} and k_{cross}' cross-relaxation rates can be strongly different.

Effective Two-Site Model. Since in a four-site model the general solution of modified Bloch equations strongly inflates the number of adjustable parameters, we reduced this number by introducing an effective two-site model.[3] In this simplified model the four different couplings of a genuine four-site case will be represented by the nonequivalence of the effective sites. Then, unlike the case for mirror conformers, different pairs of phosphorus and nitrogen couplings, and even different relaxation parameters, can characterize the sites between which exchange takes place. Furthermore in this model, the multiplicity of exchange processes will be represented by a cross-relaxation term between phosphorus spins. According to this last assumption, in the coalescence regime only one exchange process could produce special line shape, while broadening due to additional exchange processes contributes to the δH line width of the basic Lorentzian curve through the γ'' cross term (eq (1)):

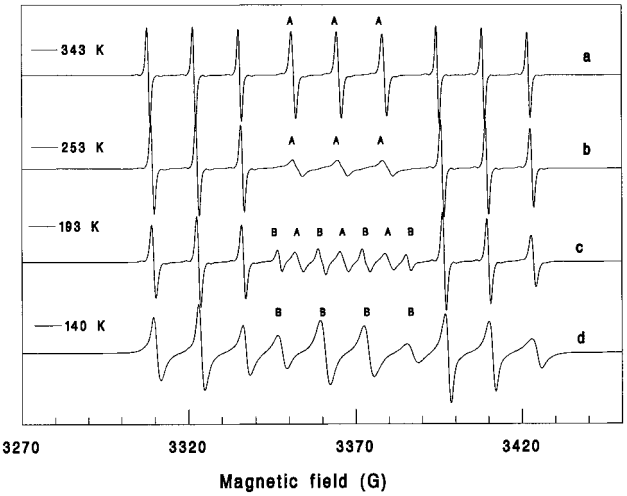

Figure 4. Calculated ESR spectra for radical **3**: (a) 343 K, (b) 253 K, (c) 193 K and (d) 140 K.

$$\delta H = \alpha + \beta M_1 + \gamma M_1^2 + \beta'(M_2 + M_3) + \gamma' M_1(M_2 + M_3) + \gamma'' M_2 M_3 \quad (1)$$

Here M_1, M_2, and M_3 stand for the magnetic quantum numbers of nitrogen and of the two phosphorus nuclei, respectively. The effective sites may have different sets of line width parameters α, β, γ, β', γ', and γ'' (eq 1), and their coupling constants and g values are population weighted averages over the conformers involved in the secondary exchange.

Parameter Adjustments. *Spectrum Simulations for Radical **3**.* For radical **3**, 10 parameters (the g factor, three hyperfine couplings, and six relaxation parameters) for each effective site have to be adjusted. Furthermore, the correlation time and the relative conformer population should also be considered; then finally with everything included 22 parameters have to be adjusted. However, when the number of parameters is large compared to the number of experimental data, a satisfactory optimization of a curve can be obtained with a meaningless set of parameters.[6] Except in the coalescence region, each ESR line can be characterized by two experimental parameters: its position and its width. However, for nitrogen couplings only two out of the three line positions are independent. Consequently, in the fast exchange limit no more than 15 parameters could be determined. The number of parameters was reduced either by assuming that all the relaxation coefficients are the same for the two sites or that the effective sites are mirror images. In the former approach 15 parameters remain depending on the inclusion of the γ'' cross relaxation term, while when the effective sites are considered as mirror images, the number of parameters is halved to 11.

The qualitative features of the spectra were very well reproduced (Figure 4) either with the 15- or the 22-parameter optimization (the simulations shown in Figure 4 were obtained with the former choice). In both cases the standard deviation was almost the same above 233 K, while below this temperature a small increase (not larger than 2) was found using 15 parameters. The use of 11 parameters for the calculation gave a qualitatively good fit only above 253 K; at lower temperature

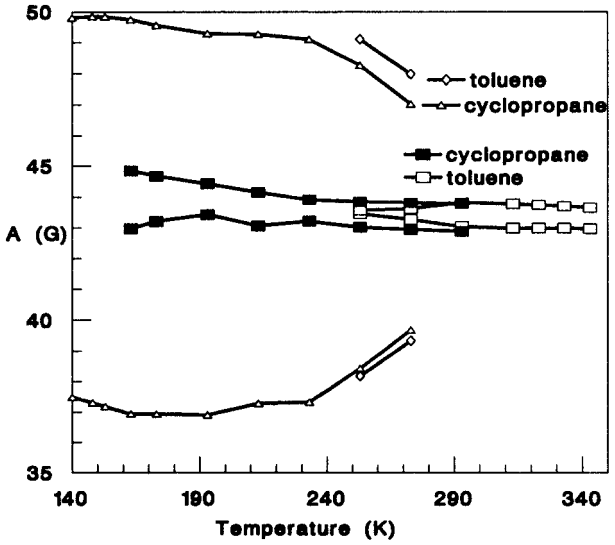

Figure 5. Phosphorus hyperfine couplings for radical **3** in toluene and cyclopropane as a function of temperature. The squares indicate values assigned to the open conformers, while the triangles and diamonds represent data for the locked conformers.

incorrect results were obtained, since the B type lines could not be fitted adequately. The calculated phosphorus coupling constants for the two sites are shown in Figure 5. The couplings giving rise to the A lines exhibited only a small difference over the whole temperature range; however, significantly different hyperfine coupling values, typical of axial and equatorial phosphorus nuclei, were obtained in order to fit the B lines.

The exchange frequency and the populations of the different sites could not be established accurately near the fast exchange limit. The experimentally available quantities are the δH line broadening and the h_{av} line positions, which can be expressed as

$$\delta\mathrm{H} = 4p_1p_2(h_1 - h_2)^2/k \qquad (2)$$

$$h_{av} = p_1h_1 + p_2h_2 \qquad (3)$$

where h_1 and h_2 indicate the line positions in site 1 and site 2, and p_1, p_2 ($p_1 + p_2 = 1$) stand for the populations. The populations and the k value can be determined if we can measure h_1 and h_2 from spectra recorded in the slow exchange limit. For an exact four-site model, however, there are four different exchange processes that can contribute to the line broadening.[3f] To simplify the analysis, we have already introduced an effective relaxation coefficient γ'', which was neglected when we analyzed the temperature dependence of the primary exchange rate. Thus for radical **3**, we also carried out the optimizations using 15 parameters in the calculations.

Spectrum Simulation for Radical 2. For radical **2** two additional proton couplings should be determined for each effective site, and in this model 26 parameters are involved in the calculations. We again simplified the optimization procedure assuming the same relaxation parameters for both sites (20 parameter adjustment), and a reliable fit was expected, since there are 27 well-resolved lines in the spectra representing 27 independent line widths and 18 positions. Excellent fits were obtained over the entire temperature range investigated (Figure 3). The calculated phosphorus and proton couplings are shown in Figure 6. In the high-temperature region the effective sites seem to be equivalent, since only two significantly different couplings are obtained, while below 250 K the two sites are characterized by two markedly different pairs of couplings. For site double-prime both proton and phosphorus couplings differ

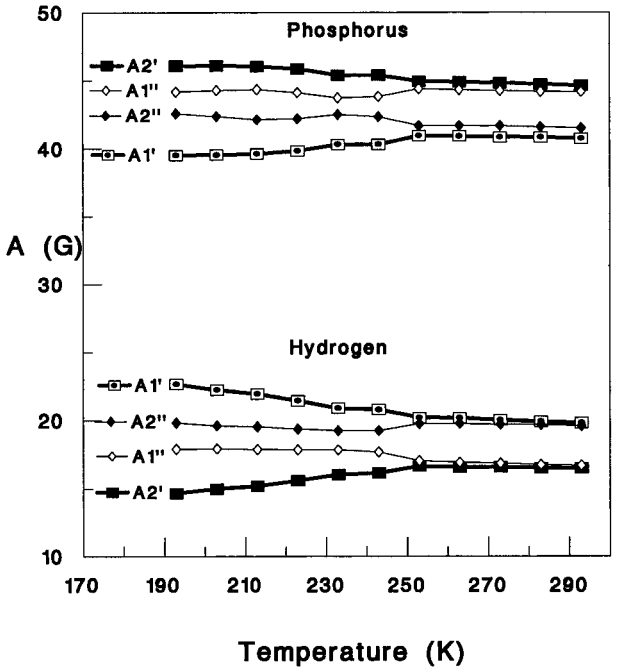

Figure 6. Phosphorus and hydrogen hyperfine couplings for radical **2** in dichoromethane as a function of temperature. Thick lines: locked molecules. Thin lines: open molecules.

only slightly (1−2 G), while for site prime larger differences (7−9 G) are obtained (Figure 6).

Superposition Model for Exchange. Below 253 K the spectra of radical **3** consist of the superimposed A and B patterns, where only the A lines seem to be affected by an exchange broadening. In this case, the four-site exchange can be considered as composed of two separated pairs of conformers, one that exhibits chemical exchange and one that does not. While previously we described the *interconversion between these pairs of conformers* by the primary exchange process, we will now neglect any interconversion between the pairs and consider only *exchange within one of the pairs*. The B set of lines was simulated by using the rigid limiting case with nonequivalent phosphorus nuclei. Nine parameters were adjusted: the g factor, the couplings for one nitrogen and two phosphorus, and five relaxation parameters. To simulate the A set of lines, an exchange model including 15 parameters was used (the γ'' cross relaxation factor was neglected). Altogether, we optimized 24 parameters, but kept δH in eq 2 as independent of temperature. Then the number of adjustable parameters is just compatible with the information content of spectra (at low temperature 13 well-resolved lines can be detected). The quality of the fit was still good if we assumed that the exchange takes place between mirror conformers (19 parameters optimization); however the standard deviation was increased by a factor between 2 and 3. Since the line width broadening due to the exchange depends on the square of the coupling constant differences, we fixed the couplings and corrected all k values using eq 2. This correction makes the absolute value of k reported in Figure 7 more uncertain, but its variation with the temperature becomes more reliable. The exchange rates obtained by analogous computation for radical **2** are shown in Figure 8.

Discussion

Conformational Assignments. *Radical 3.* Chemical exchange takes place at high temperature between conformers characterized by slightly different phosphorus couplings. The

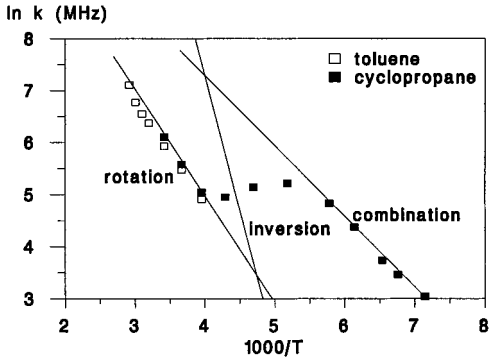

Figure 7. Arrhenius plot of effective exchange frequency calculated for radical **3**. The dominant contributions from rotations and combined motion are indicated.

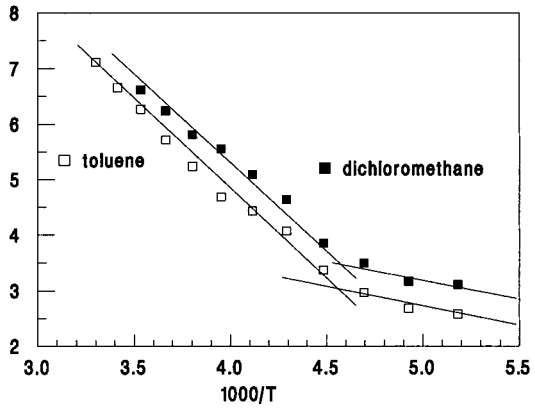

Figure 8. Arrhenius plot of effective exchange frequency calculated for radical **2**. The dominant contributions from rotations and ring inversion are indicated.

magnitude of the coupling constants is intermediate between those determined for typical axial and equatorial phosphorus nuclei in **3B** or in single phosphoryl substituted pyrrolidinoxyl radicals. Ring inversion can effectively average out the axial and equatorial splittings, and line broadening is mainly caused by hindered rotations around the C−P bonds (eq 4):

$$\{Q^+, R^+\} \Leftrightarrow \{Q^-, R^-\} \quad (4)$$

When the variation of the exchange frequency is plotted versus the temperature (Arrhenius plot, Figure 7), the high-, low-, and intermediate-temperature regions are clearly distinguished. In the high-temperature region a good linear correlation is observed with a slope corresponding to $\Delta E = 17$ kJ/mol, and $A = 4 \times 10^{11}$ s^{-1}. This energy can be assigned to the barrier of gear rotations around the C−P bonds.

The intermediate-temperature region shows a nonlinear Arrhenius plot and, as already mentioned, is characterized by the appearance of the B lines arising from strongly different phosphorus couplings. These lines are already narrow at 233 K with intensities that are small compared to those of the A lines. The B lines were attributed to molecules locked in conformations denoted by Q^- and R^+. Since in the temperature range 158−233 K the A lines are also present (Figure 1), a portion of the molecules should still give rise to fast ring inversion. We will call these molecular conformations the open Q^+ and R^- sites:

$$Q^+ \Leftrightarrow R^- \quad (5)$$

When the Q^- and R^+ conformations are locked, interconversion between open Q^+ and R^- sites can only take place through a combined intramolecular motion in which carbon−phosphorus bond rotations and ring inversion occur simultaneously. We assign the low-temperature region of the Arrhenius plot in Figure 7 to this combined exchange, for which we extract an activation energy of 11 kJ/mol and a preexponential factor of 3×10^{11} s^{-1}.

TABLE 1: EPR Parameters, Potential Barriers, and Arrhenius Preexponential Factors for Radicals 1−3

parameter	unit	**1**[a,d]	**2A**[b,e,g]	**2B**[b,e]	**3A**[c,f,h]	**3B**[c,f]
a_N'	G	13.30	14.10	14.10	13.52	13.52
a_N''	G	13.30	13.97	13.97	13.30	13.30
$a_P(1)$	G	51.00	44.2	46.1	43.4	49.3
$a_P(2)$	G	51.00	42.6	39.5	44.4	36.9
$a_H(1)$	G		17.9	14.7		
$a_H(2)$	G		19.8	22.7		
a_α^{13C}	G	6.4	5.9		5.7	
a_β^{13C}	G	5.0			6.8	
$\Delta\epsilon_a$	kJ/mol		27[h]	6[i]	17[h]	11[i]
A	s^{-1}		2×10^{13} [j]		4×10^{11} [k]	3×10^{11} [l]

[a] Optimization without exchange. [b] 20-parameter fit. [c] 16-parameter fit. [d] At 273 K in toluene. [e] At 193 K in dichloromethane. [f] At 193 K in cyclopropane. [g] Long-range couplings: $a_{\gamma H}(4) = 0.39$ G. [h] High-temperature limit. [i] Low-temperature limit. [j] For ring inversion. [k] For rotations around the C−P bonds. [l] For combined exchange.

The intermediate temperature region of the Arrhenius plot shows an unexpected acceleration for the exchange rate which is faster between 213 and 193 K than at 253 K. This anomaly cannot be accounted for by any uncertainty in the exchange rate values, and it could be explained as follows. At high temperature fast ring inversion will not generate any broadening, and only the much slower rotation could broaden the lines and determine the effective exchange rate. Below 253 K, the rotations become too slow to generate line broadening, while the exchange between the open molecular conformations (Q^+ and R^-) is still rather fast and generates only a small line broadening. Below 193 K the exchange between the open molecules reaches the critical frequency domain, where it will strongly broaden the A lines.

Interesting thermodynamic considerations can also be derived from the Arrhenius plot. Since ring inversion has a much larger potential barrier (ca. 27 kJ/mol, Table 1) than the coupled motion (ca. 11 kJ/mol, Table 1), at low temperature the coupled motion interconverting Q^+ and R^- might be favored compared to the interconversion involving successive inversion and rotation: $Q^+ \Leftrightarrow R^+ \Leftrightarrow R^-$. However, at high temperature the coupled motion will lose its importance due to its small entropy compared to the large entropy of ring inversion.

Radical 2. For radical **2** the Arrhenius plot of exchange rate deviates from linearity in the low-temperature region (Figure 8). Presumably the different conformational behavior of radicals **2** and **3** is a consequence of the less strongly hindered rotation of geminal phosphoryl groups for the former. The broadening is then caused primarily by ring inversion, and a potential barrier of 27 kJ/mol can be extracted from the high-temperature regime. The identical pairs of coupling constants found for the effective sites (Figure 6) also support a fast averaging of rotational states. Due to the large barrier of inversion, at low-temperature rotations around the C−P bonds became the predominant line-broadening mechanism. In this case four different phosphorus and four different hydrogen couplings were needed to calculate the ESR spectra, and a small potential barrier on the order of 6 kJ/mol was estimated in the low-temperature limit.

Conclusions

The three investigated diphosphoryl-substituted pyrrolidinoxyl radicals reveal rather different molecular dynamics. The trans stereochemistry for **1** imposes a molecular geometry where both phosphoryl groups possess axial positions and no ring inversion occurs. Due to the rather free rotation around the C−P bonds,

chemical exchange cannot be detected at all. Marked chemical exchange, however, was found for the geminal substituted radicals **2** and **3**. Furthermore, for these radicals the molecular dynamics is significantly different due to the steric effect of 5,5-dimethyl substituents, which, in the case of **3**, can strongly hinder the gear motion of phosphoryl groups. In radical **2** the rotation around the C−P bonds is almost free, and at high temperature the observed chemical exchange can be assigned to ring inversion. The presence of two phosphorus substituents allows one to determine a fast inversion rate on the order of 10^{10} Hz, a potential barrier of 27 kJ/mol, and a prexponential factor of 2×10^{13} s^{-1}. At low temperature, hindered rotations around the C−P bonds become the predominant broadening mechanism, and a potential barrier of 6 kJ/mol can be estimated.

Radical **3** presents a very complex kind of exchange phenomenon never reported in the literature even for the cases involving exchange among four different sites.[4] At 273 K hindered rotations around the C−P bonds can lock a portion of the molecules in a geometry exhibiting slightly different phosphorus couplings. Above this temperature rotations around the C−P bonds produce chemical exchange between effective sites, which are both composed of two rapidly interconverting ring conformers. The barrier of rotation is estimated to be 17 kJ/mol and is substantially larger than that found for radical **2**. Below 253 K the ESR spectra of radical **3** clearly show the presence of two types of molecules exhibiting strongly different dynamic properties. One portion of the molecules is locked and shows neither rotations around the C−P bonds nor ring inversion on the ESR time scale. The phosphoryl groups are frozen in axial and equatorial positions, and the markedly different phosphorus couplings give rise to the B lines. The other portion of the molecules that can be classified as "open" still produces exchange via a combined motion involving simultaneous ring inversion and rotations around the C−P bonds. The estimated barrier of the combined interconversion is 11 kJ/mol. The concentration of "open" molecules decreases with temperature, and below 153 K only "locked" molecules exist.

For radical **2** we could also observe the simultaneous existence of the "open" and "locked" molecules below 200 K. The ring geometry for "locked" molecules seems to be different for **2** and **3**. For **3** the large difference in the phosphorus couplings indicates a distortion of $^3T_4$ twist conformer toward the ^3E envelope, and the phosphorus nuclei which are pseudoaxial and pseudoequatorial in the former will become axial and equatorial in the latter. In the case of **2** the coupling constants of "locked" states have a much smaller difference, the proton couplings showing a larger variation than the phosphorus couplings. This indicates that **2** has a geometry in which the ring is less puckered and the twist conformation is distorted in the direction of an E_4 envelope.

Experimental Section

5,5-Dimethyl pyrroline-*N*-oxide (DMPO) was purchased from Aldrich Chemical Co. THF was distilled under nitrogen over sodium and benzophenone prior to use. ESR measurements were performed on a Bruker ESP 300 spectrometer equipped with a TM110 cavity and a X-band resonator (9.41 GHz). All ESR spectra were recorded at 100 kHz magnetic field modulation.

The ESR samples were deoxygenated by freeze and thaw cycles.

Synthesis. *Diethyl(5,5-dimethyl-1-oxide pyrrolidin-2-yl)-phosphonate, **5***. A solution of DMPO (**4**) (1 g, 8.8 mmol) and diethyl phosphite (6.5 g, 47.1 mmol) in dry THF (30 mL) was refluxed under nitrogen for 18 h. After removal of the solvent, the product was diluted with dichloromethane, washed with water, and dried over sodium sulfate. After filtration and concentration, the hydroxylamine was dissolved in methanol (50 mL) and oxidized in the presence of cupric(II) acetate (50 mg, 20 min, room temperature). The methanol was removed under vacuum, and the product was chromatographied by preparative TLC over silicagel using dichloromethane/ethanol (99/1 v/v) as eluent to yield 14% (0.31 g, 1.24 mmol) of pure nitrone **5**. The ^{1}H and ^{13}C NMR data were in accordance with the data previously reported.[7] ^{31}P NMR (40.5 MHz) ($CDCl_3$) δ (ppm) 4.59.

ESR Experiments. *2,2-Bis(diethoxyphosphoryl)pyrrolidinoxyl, **2***. Pyrrolidine, **6** (10.3 mg, 0.03 mmol) was dissolved in 0.1 mL of solvent, and *m*-CPBA (7.2 mg, 0.03 mmol) was added. The mixture was then poured in an ESR tube, and the oxygen was removed by freeze and thaw cycles.

*2,2-Bis(diethoxyphosphoryl)-5,5-dimethylpyrrolidinoxyl, **3***. A solution of nitrone **5** (30 mg, 0.12 mmol) and diethyl phosphite (0.1 mL, 0.77 mmol) in toluene was heated 30 min at 70 °C under air bubbling. At 0 °C, *m*-CPBA (3.5 mg, 0.01 mmol) was added. The solution was then poured in an ESR tube, and oxygen was removed by freeze and thaw cycles. For spectra in the low-temperature range, the toluene was removed under vacuum and the tube filled with cyclopropane.

*2,5-Bis(diethoxyphosphoryl)-2,5-dimethylpyrrolidinoxyl, **1***. Pure nitroxide **1** was prepared from the pyrrolidine **7** according to a procedure that will be published elsewhere. The preparation of the ESR samples was the same as for the other nitroxides.

The ESR spectra of radicals **1**, **2**, and **3** were recorded in toluene between 193 and 343 K, while radicals **2** and **3** were also investigated in dichloromethane and cyclopropane, respectively.

Acknowledgment. This work was supported by Grant OTKA (Hungarian National Research Fund) T-015841.

References and Notes

(1) (a) Tordo, P; Boyer, M.; Santero, O.; Pujol, L. *J. Phys. Chem.* **1978**, *82*, 1742. (b) Mercier, A.; Berchadsky, Y.; Badrudin; Pietri, S.; Tordo, P. *Tetrahedron Lett*. **1991**, *32*, 2125−2128. (c) Le Moigne, F.; Mercier, A.; Tordo, P. *Tetrahedron Lett.* **1991**, *32*, 3841−3844. (d) Dembkowski, L.; Finet, J. P.; Fréjaville, C.; Le Moigne, F.; Maurin, R.; Mercier, A.; Pages, P.; Stipa, P.; Tordo, P. *Free Rad. Res. Commun.* **1993**, *19*, S23−S32. (e) Stipa, P.; Finet, J. P.; Le Moigne, F.; Tordo, P. *J. Org. Chem.* **1993**, *58*, 4465−4468.

(2) (a) Fréjaville, C.; Karoui, H.; Le Moigne, F.; Culcasi, M.; Pietri, S.; Tordo, P. French Patent No. PV 9308906, 20 July, 1993. (b) Fréjaville, C.; Karoui, H.; Tuccio, B.; Le Moigne, F.; Culcasi, M.; Pietri, S.; Lauricella, R.; Tordo, P. *J. Chem. Soc., Chem. Commun.* **1994**, 1793−1794. (c) Fréjaville, C.; Karoui, H.; Tuccio, B.; Le Moigne, F.; Culcasi, M.; Pietri, S.; Lauricella, R.; Tordo, P. *J. Med. Chem.* **1995**, *38*, 258−265. (d) Tuccio, B.; Lauricella, R.; Frejaville, F.; Bouteiller, J. C.; Tordo, P. *J. Chem. Soc., Perkin Trans. 2* **1995**, 295−298.

(3) (a) Bolton, J. R.; Carrington, A. *Mol. Phys*. **1962**, 5, 161. (b) Carrington, A. *Mol. Phys*. **1962**, 5, 425. (c) Bolton, J. R.; Carrington, A.; Todd, P. F. *Mol. Phys*. **1963**, 6, 169. (d) Yamakazi, I.; Piette, L. H. *J. Am. Chem. Soc*. **1965**, 87, 986. (e) Smith, I. C. P.; Carrington, A. *Mol. Phys*. **1967**, 12, 439. (f) Loth, K.; Graf, F.; Günthard, Hs. H. *Chem. Phys*. **1976**, 13, 95−113,

(4) Rockenbauer, A.; Korecz, L.; Hideg, K. *J. Chem. Soc., Perkin Trans 2* **1993**, 2149−2156.

(5) Carrington, A.; McLachlan, A. D. *Introduction to Magnetic Resonance;* Harper & Row: London, 1969; Chapter 12.

(6) Rockenbauer, A.; Korecz, L. *Appl. Magn. Reson*. **1996**, *10*, 29−43.

(7) Janzen, E. G.; Zhang, Y.-K. *J. Org. Chem*. **1995**, *60*, 5441−5445.